EPJ manuscript No.
(will be inserted by the editor)

Freak waves in laboratory and space plasmas

Freak waves in plasmas

Michael S. Ruderman,[a]

School of Mathematics and Statistics, University of Sheffield, Hounsfield Road, Hicks Building, Sheffield, S3 7RH, UK

Abstract. Generation of large-amplitude short-lived wave groups from small-amplitude initial perturbations in plasmas is discussed. Two particular wave modes existing in plasmas are considered. The first one is the ion-sound wave. In a plasmas with negative ions it is described by the Gardner equation when the negative ion concentration is close to critical. The results of numerical solution of the Gardner equation with the modulationally unstable initial condition are presented. These results clearly show the possibility of generation of freak ion-acoustic waves due to the modulational instability. The second wave mode is the Alfvén wave. When this wave propagates at a small angle with respect to the equilibrium magnetic field, and its wave length is comparable with the ion inertia length, it is described by the DNLS equation. Studying the evolution of an initial perturbation using the linearized DNLS equation shows that the generation of freak Alfvén waves is possible due to linear dispersive focusing. The numerical solution of the DNLS equation reveals that the nonlinear dispersive focusing can also produce freak Alfvén waves.

1 Introduction

Freak (or rogue, or giant) waves are extremely violent phenomena in the ocean. An encounter with such a wave can be fatal even for big ocean liners. These waves can be also very dangerous for various hydrotechnic constructions. This makes studying freak waves a very important problem. Hence, it is not surprisings that the phenomenon of freak waves has attracted ample attention of oceanographers (see, e.g., [1–7]).

It seems that the phenomenon of freak waves is quite universal and occurs not only in the ocean. Recently it has been found experimentally that freak waves can be generated in optical systems [8,9].

Large-amplitude waves are also observed in space plasmas. In Fig. 1 taken from Ref. [10] the observations of spike-like dips in the interplantary magnitic filed called magnetic holes are shown. This observations were made by Voyager 1 in the heliosheath, which is a region between the termination shock, where the solar wind plasma is decelerated, and the heliopause separating the solar wind from the interstellar medium. This region is situated at about 100 astronomical units from the sun.

At present there are a few competing theories explaining the appearance of magnetic holes. They include the current sheet model [11], the creation of magnetic holes by the mirror instability [12–14], and the soliton model [15]. We can suggested one more model explaining the existence of magnetic holes: they can be freak waves. This is only one example from space

[a] e-mail: M.S.Ruderman@sheffield.ac.uk

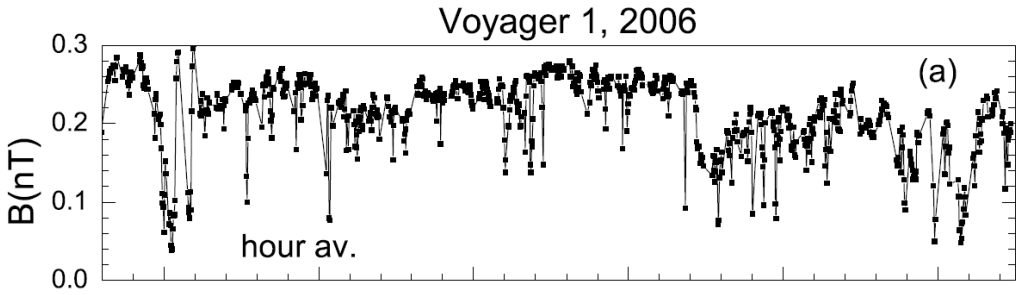

Fig. 1. Voyager 1 observations of hour averages of the magnetic field strength B in the heliosheath. The magnetic field magnitude shows many spike-like dips that are too narrow to be resolved in the hour average. Figure taken from Ref. [10]

physics where the theory of freak waves can be applied, but it clearly shows that freak waves in plasmas are worth of studying.

In this paper we give a brief review of recent progress in studying generation of freak waves in plasmas. The paper is organized as follows. In the next section we consider generation of freak waves in plasmas with negative ions. The evolution of wave packets in such plasmas is described by the Gardner equation. In Sect. 3 we discuss the generation of Alfvén freak waves described by the the Derivative Nonlinear Schrödinger (DNLS) equation. Sect. 4 contains the summary of the review and our conclusions.

2 Modulationally unstable ion-acoustic waves in plasmas with negative ions

2.1 Gardner equation for nonlinear waves

Nonlinear ion-acoustic waves in plasmas have been studied for a very long period of time. It was shown that the Korteweg-de Vries (KdV) equation can be used to describe waves with moderate amplitudes [16–18]. The KdV-type ion-acoustic solitons in plasmas consisting of electrons and positive ions were then studied experimentally [19–23].

The behaviour of ion-acoustic waves becomes mode complicated when the plasma contains not only positive but also negative ions. When the concentration of negative ions is equal to the critical value, the coefficient at the nonlinear term in the KdV equation is equal to zero, which implies that the cubic non-linearity has to be takes into account. As a result, nonlinear ion-acoustic waves in plasmas with the critical concentration of negative ions are described by the modified Korteweg-de Vries (mKdV) equation [24–28]. The mKdV solutions were also observed in the experiment [29].

When the negative ion concentration is not exactly equal to the critical value, but close to it, both the quadratic and cubic non-linearity has to be taken into account. In that case the dynamics of nonlinear ion-acoustic waves is described by the Gardner equation [30,31],

$$\frac{\partial\psi}{\partial\tau} - a\psi\frac{\partial\psi}{\partial\xi} + g\psi^2\frac{\partial\psi}{\partial\xi} + \chi\frac{\partial^3\psi}{\partial\xi^3} = 0. \tag{1}$$

Here ψ is the dimensionless electric potential, τ the dimensionless time, and ξ the dimensionless spatial variable in the reference frame moving with the velocity of long linear ion-acoustic waves with respect to the rest plasma. The coefficients in Eq. (1) are given by

$$a = \frac{\gamma(\eta+1)\sqrt{6(3\eta^2-2\eta+3)}}{\eta^{1/2}[3\eta-3+\sqrt{3(3\eta^2-2\eta+3)}]^{3/2}}, \tag{2}$$

$$g = \frac{\sqrt{6}[3(5\eta^2 - 6\eta + 5) - 5(\eta - 1)\sqrt{3(3\eta^2 - 2\eta + 3)}]}{3\eta[\sqrt{3(3\eta^2 - 2\eta + 3)} - 3\eta + 3]^{1/2}}, \tag{3}$$

$$\chi = \left(\frac{3\eta - 3 + \sqrt{3(3\eta^2 - 2\eta + 3)}}{8\eta}\right)^{1/2}, \tag{4}$$

where $\eta = Z_+ m_- / Z_- m_+$, γ the dimensionless parameter proportional to the deviation of the negative ion density from the critical value, m_+ and m_- are the masses of the positive and negative ions, and Z_+ and Z_- are the ratios of the electrical charges of the positive and negative ions to the elementary charge.

2.2 Dynamics of modulationally unstable ion-acoustic waves

When the negative ion density is equal to the critical values, which corresponds to $\gamma = 0$, Eq. (1) reduces to the mKdV equation. The dynamics of modulationally unstable packets described by the mKdV equation has been extensively studied (see, e.g., [32]). Recently a similar study has been carried out for modulationally unstable packets described by the Gardner equation [31]. Here we describe the most important results obtained in [31] that are related to the generation of freak waves.

We start from discussing the modulational instability of weakly nonlinear wave packets described by Eq. (1). We consider the solution to Eq. (1) in the form of weakly modulated sinusoidal wave,

$$\psi(\xi, \tau) = \varepsilon \Psi(X, T) \exp(i\Theta) + \text{c.c.}, \tag{5}$$

where $X = \varepsilon(\xi + 3\chi k^2 \tau)$, $T = \varepsilon^2 \tau$, $\Theta = k\xi - \omega\tau$, k is the carrier wavenumber, $\omega = -\chi k^3$, ε is an arbitrary small parameter, and c.c. denotes the complex conjugate. The evolution of the complex amplitude Ψ is described by the nonlinear Schrödinger equation [33,34],

$$i\frac{\partial \Psi}{\partial T} = 3\chi k \frac{\partial^2 \Psi}{\partial X^2} + \delta k |\Psi|^2 \Psi, \tag{6}$$

where

$$\delta = g - \frac{a^2}{6\chi k^2}. \tag{7}$$

Equation (6) has the solution in the form of a monochromatic wave given by

$$\Psi = \Psi_0 \equiv A_0 \exp[i(KX - \Omega T)], \quad \Omega = k(\delta A_0^2 - 3\chi K^2). \tag{8}$$

It is straightforward to show that this solution is stable when $\chi\delta < 0$, and unstable when $\chi\delta > 0$. This is the well-known criterion for the modulational or Benjamin-Feir instability (see, e.g., [35], [36]). Since $\chi > 0$, the stability of monochromatic ion-acoustic waves is determined by the sign of δ. It follows from Eq. (7) that the condition for the onset of the modulational instability is

$$k > k_c = \frac{|a|}{\sqrt{6g\chi}}. \tag{9}$$

In a particular case when the negative ion density is equal to its critical value, i.e. $\gamma = 0$, we have $a = 0$ and the monochromatic wave is unstable for any value of k. In the general case this wave is unstable only if the carrier wavenumber k is sufficiently large. Only the long-wavelength perturbations with the modulation wave number κ satisfying

$$\kappa < \kappa_{\text{lim}} = A_0 \sqrt{\frac{2\delta}{3\chi}} \tag{10}$$

are unstable.

The dynamics of the modulationally unstable wave packets was studied numerically. To do this the new variables were introduced,

$$\Upsilon = -(g/6)^{1/2}\chi^{-1/6}\psi\,\mathrm{sgn}(a), \qquad \zeta = \chi^{-1/3}\xi. \tag{11}$$

In the new variables Eq. (3) reduces to

$$\frac{\partial\Upsilon}{\partial\tau} + 6\alpha\Upsilon\frac{\partial\Upsilon}{\partial\zeta} + 6\Upsilon^2\frac{\partial\Upsilon}{\partial\zeta} + \frac{\partial^3\Upsilon}{\partial\zeta^3} = 0, \tag{12}$$

where $\alpha = |a|(6g)^{-1/2}\chi^{-1/6}$. The criteria for the modulational instability are transformed to

$$k > \alpha, \qquad \kappa < 2A_0\sqrt{1-\frac{\alpha^2}{k^2}}. \tag{13}$$

Equation (12) was solved numerically using the finite-difference scheme described in [37]. The initial condition was taken in the form of a modulated harmonic wave,

$$\Upsilon = A[1 - m\cos(\kappa\zeta)]\sin(k\zeta). \tag{14}$$

Note that, in accordance with Eqs. (5) and (8), $A = 2A_0$. The main purpose of the study was to investigate the role of the quadratic non-linearity. In accordance with this the calculations were carried out with $\alpha = 1$ and $\alpha = 0$ (corresponding to the mKdV equation), and then the results were compared. In all calculations $m = 0.05$, $k = 1.256$ and $\kappa = 0.0157$ were taken. In particular, this implies that the first inequality in (13) was satisfied for both values of α. Figure 2 shows the time evolution of the wave for $A = 0.05$. For this value of A the second inequality in Eq. (13) is satisfied, so that the perturbation with $k = 1.256$ is unstable. In Fig. 2 we clearly see the formation of wave groups with the amplitudes approximately equal to 0.15, which is three times larger than the initial amplitude.

Figure 3 shows the time evolution of the wave for $A = 0.23$. Once again the second inequality in Eq. (13) is satisfied, so that the perturbation with $k = 1.256$ is unstable. In this figure we also can see the formation of wave groups with the amplitudes a few times larger than the initial one.

Hence, the results of numerical modelling reveal that the freak waves are formed due to modulational instability both in the case of purely cubic non-linearity (mKdV equation) and mixed non-linearity (Gardner equation). These waves exist only for short periods of time and then disappear. The main role of the quadratic non-linearity is that it decelerates the wave evolution. As a result, the first freak wave appears later in the case of mixed non-linearity than in the case of purely cubic non-linearity.

3 Generation of large-amplitude magnetohydrodynamic pulses by dispersive focusing

3.1 Derivative Nonlinear Schrödinger equation for Alfvén waves

The Derivative Nonlinear Schrödinger (DNLS) equation describes propagation of nonlinear Alfvén waves in plasmas [38–41]. It can be written in the form

$$\frac{\partial b}{\partial t} + h\frac{\partial}{\partial x}(|b|^2 b) + i\lambda\frac{\partial^2 b}{\partial x^2} = 0. \tag{15}$$

Here $b = B_y + iB_z$, where B_y and B_z are the y and z-components of the magnetic field,

$$h = \frac{V_A}{4B_x^2(1-\beta)}, \;\; \lambda = \frac{V_A^2}{2\Omega_i}, \;\; V_A^2 = \frac{B_x^2}{\mu_0\rho_0}, \;\; \Omega_i = \frac{eB_x}{m_i},$$

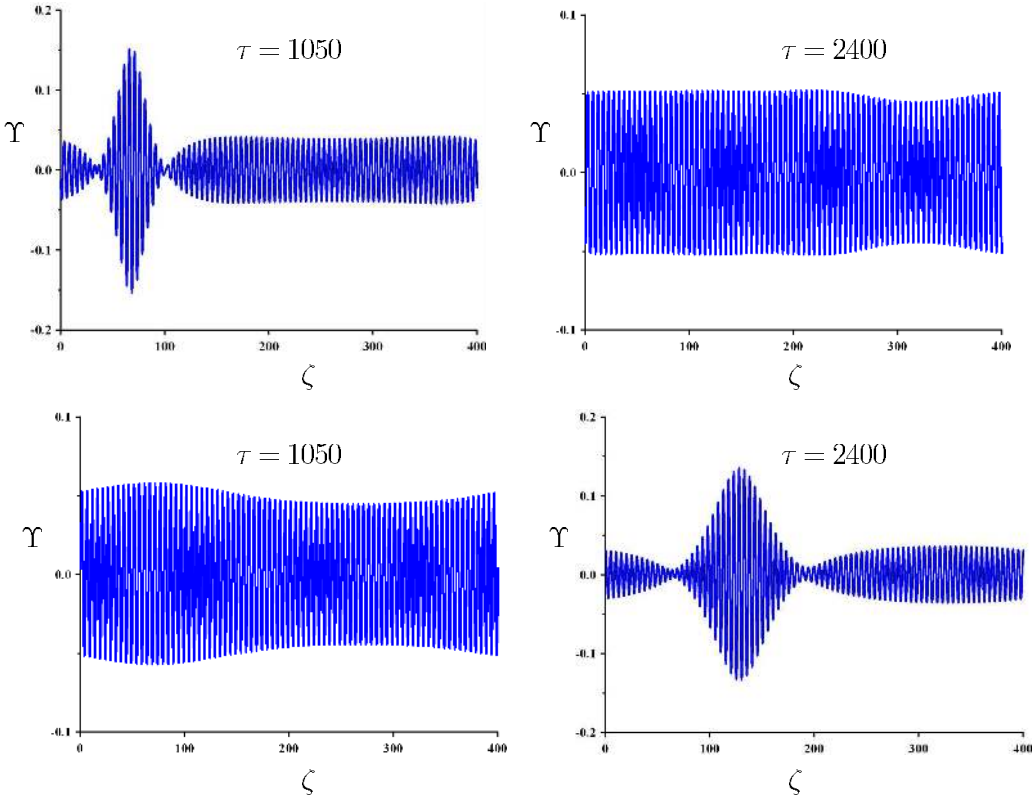

Fig. 2. Formation of the first intense wave groups due to modulational instability of the wave with the initial amplitude $A = 0.05$. The upper panels correspond to $\alpha = 0$ (the mKdV equation), and the lower to $\alpha = 1$ (the Gardner equation). Figure taken from Ref. [31]

B_x is the x-component of the magnetic field (which remains constant), β is the square of the ratio of the sound speed c_S to the Alfvén speed V_A, and Ω_i is the ion gyrofrequency; μ_0, e and m_i are the magnetic permeability of free space, the elementary charge, and the ion mass, respectively. Note that Eq. (15) is written in the reference frame moving with the speed V_A in the positive x-direction with respect to the rest plasma.

The DNLS equation has been derived under the assumption that the non-linearity and dispersion are small. These two conditions mean that $|b| \ll B_x$, and that the characteristic spatial scale of the perturbation variation is much large than the ion inertial length $\sqrt{m_i/\mu_0 n_i e^2}$, where n_i is the concentration of ions. Another assumption made when deriving the DNLS equation is that the waves propagate at a small angle with respect to the equilibrium magnetic field. A comparison of the theoretical results obtained on the bases of the DNLS equation with the observational data shows that, very often, the DNLS equation provides fairly good description of Alfvén waves in the solar wind [42].

3.2 Generation of large-amplitude pulses described by the DNLS equation

Recently the generation of large-amplitude short-lived Alfvénic pulses described by the DNLS equation has been studied [43]. In what follows we will briefly describe the results of this study. Let us first consider the linearized DNLS equation. Then we obtain Eq. (15) with the nonlinear term neglected. The solution to this equation satisfying the initial condition $b(0, x) = b_0(x)$ is

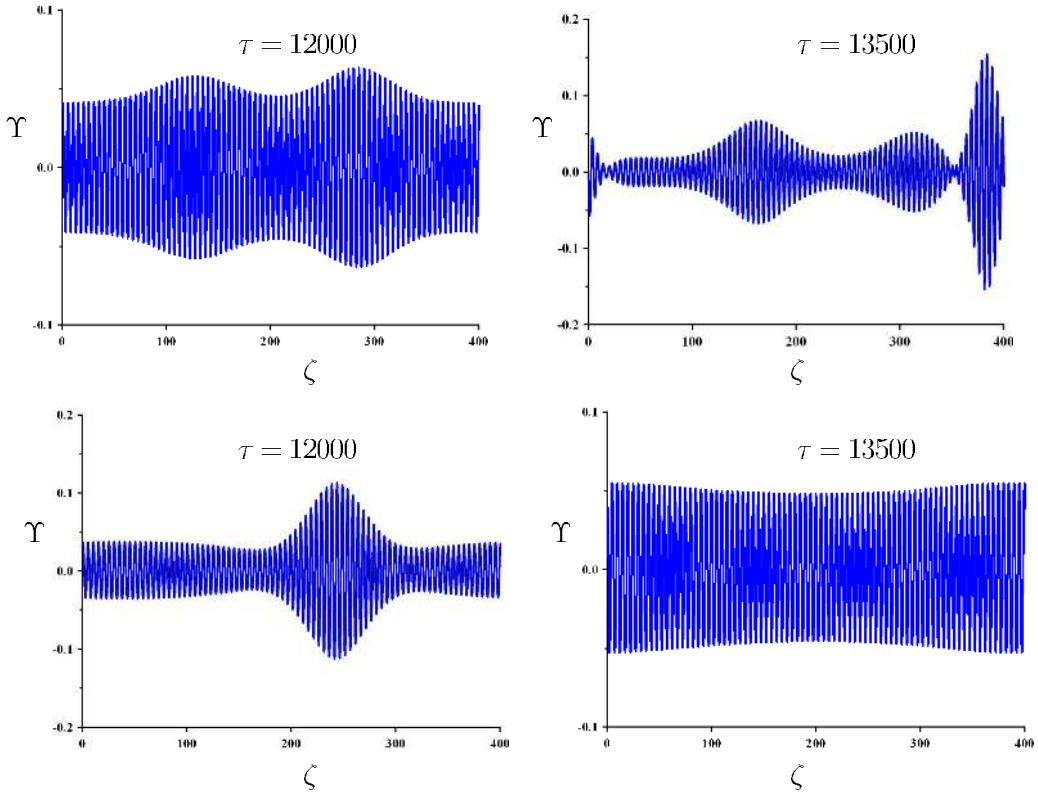

Fig. 3. Formation of the first intense wave groups due to modulational instability of the wave with the initial amplitude $A = 0.23$. The upper panels correspond to $\alpha = 0$ (the mKdV equation), and the lower to $\alpha = 1$ (the Gardner equation). Figure taken from Ref. [31]

straightforward,

$$b(t,x) = \frac{1+i}{2\sqrt{2\pi\lambda t}} \int_{-\infty}^{\infty} b_0(s) \exp\left(-\frac{i(x-s)^2}{4\lambda t}\right) ds. \tag{16}$$

Let us take the initial condition in the form

$$b_0(x) = a \exp[(-1+i\sigma)(x/l)^2], \tag{17}$$

where σ is a real constant. Substituting this expression for b_0 in Eq. (16) we immediately obtain

$$|b| = \frac{al}{[(l^2-4\lambda\sigma t)^2 + (4\lambda t)^2]^{1/4}} \exp\left(-\frac{(xl)^2}{(l^2-4\lambda\sigma t)^2 + (4\lambda t)^2}\right). \tag{18}$$

Obviously, at fixed $t > 0$, $|b|$ takes its maximum value at $x = 0$, and this maximum is given by

$$|b|_{\mathrm{M}} = al[(l^2-4\lambda\sigma t)^2 + (4\lambda t)^2]^{-1/4}. \tag{19}$$

When $\sigma < 0$, $|b|_{\mathrm{M}}$ is a monotonically decreasing function of time, so large-amplitude pulses cannot be generated. However, when $\sigma > 0$, the situation is different. Now $|b|_{\mathrm{M}}$ takes its maximum value at

$$t = t_{\max} \equiv \frac{\sigma l^2}{4\lambda(1+\sigma^2)}, \tag{20}$$

and this maximum is equal to $a(1+\sigma^2)^{1/4}$. When $\sigma \gg 1$, the ratio of the wave amplitude at $t = t_{\max}$ and $t = 0$ is approximately equal to $\sqrt{\sigma} \gg 1$, i.e. large-amplitude pulses can be generated from small-amplitude wave trains.

It is not difficult to give a physical interpretation to the obtained result. Let us take $x = x_0 + \delta x$, $|x_0| \gg l/|\sigma|$, and consider $|\delta x| \ll |x_0|$ assuming that $|\sigma| \gg 1$. Then Eq. (17) can be rewritten in the approximate form as

$$b_0 = Ae^{ik_0\delta x}, \qquad k_0 = 2\sigma x_0/l^2, \qquad A = a\exp[(-1+i\sigma)(x_0/l)^2]. \tag{21}$$

These expressions describe a circularly polarized monochromatic wave with constant amplitude $|A|$. This wave is left-hand polarized when $k_0 > 0$ ($\sigma x_0 > 0$), and right-hand polarized when $k_0 < 0$ ($\sigma x_0 < 0$). Hence, a large-amplitude wave can be generated from a small-amplitude wave train given by Eq. (17) when this wave train is locally left-hand polarized for $x > 0$ and right-hand polarized for $x < 0$, and cannot be generated in the opposite case. It is worth noting that a circularly polarized wave with constant amplitude is an exact solution of the DNLS equation. When the amplitude of such a wave is sufficiently small, this wave is modulationally unstable when it is left-hand polarized [39,41], and modulationally stable when it is right-hand polarized.

When $\sigma \gg 1$, the pulse amplitude is larger than a half of its maximum value, i.e. $|b|_{\mathrm{M}} > \frac{1}{2}a\sqrt{\sigma}$, only in a narrow time interval determined by

$$|t - t_{\max}| < \frac{l^2}{2\lambda\sigma^2} = T.$$

For $|t - t_{\max}| \gtrsim t_{\max}$, it follows from Eq. (19) that the characteristic time of variation of $|b|_{\mathrm{M}}$ is $l^2/\lambda \gg T$. This estimate reveals the short-lived character of larger-amplitude pulses, similar to one found for perturbations described by the KdV and mKdV equations [2,32].

We can give a very simple qualitative explanation why large-amplitude waves can be generated from the initial small-amplitude wave train given by Eq. (17) only when $\sigma > 0$. It follows from Eqs. (15) and (21) that the local dispersion equation takes the form $\omega = -\lambda k_0^2$, so that the local group velocity is $v_g = -2\lambda k_0$. Then, for $\sigma > 0$, $v_g < 0$ when $x > 0$, and $v_g > 0$ when $x < 0$ (recall that we use the reference frame moving with the speed V_A in the positive x-direction with respect to the rest plasma). This implies that, at the initial moment of time, the energy flux is directed towards the coordinate origin, which makes the wave amplitude at the coordinate origin growing. This is a typical picture of the linear dispersive focusing. On the other hand, for $\sigma < 0$, $v_g > 0$ when $x > 0$, and $v_g < 0$ when $x < 0$. The energy flux is directed outwards from the coordinate origin and, as a result, the wave amplitude at the coordinate origin decreases.

Now we discuss the effect of non-linearity on the dispersive focusing. The DNLS equation is a completely integrable equation and can be solved by the inverse scattering method (ISM) [44–47]. The ISM is very appropriate for calculating the asymptotic behaviour of solutions with arbitrary initial conditions. However, its applicability to studying the intermediate behaviour of solutions is restricted to the initial conditions for which the corresponding scattering problem can be solved analytically. To our knowledge, the only non-trivial exact solutions to the DNLS equation obtained so far are different kinds of the N-soliton solutions (see, e.,g., [48–51]). Since, at present, it is not clear if the scattering problem for the DNLS equation for the initial condition (17) can be solved analytically, the nonlinear evolution of this perturbation was studied numerically [43]. The evolution of the initial perturbation strongly depends on the non-linearity parameter $N = hla^2/\lambda$. For the numerical solution Eq. (15) was rewritten in terms of dimensionless variables $q = b/a$, $X = x/l$ and $T = \lambda t/l^2$. The results of the numerical solution are shown in Fig. 4 for $N = 0$ (linear theory) and $N = 0.45$. In this figure the formation of a large-amplitude short-lived pulse is clearly seen.

The numerical solution was also used to study the dependence of the maximum amplitude of the wave on σ. Similar to the linear theory, this maximum amplitude is a monotonically increasing function of σ for any value of N. On the other hand, this maximum amplitude is a monotonically decreasing functions of N for any fixed σ.

This result makes an impression that the non-linearity plays a negative role in the large-amplitude pulse generation. However in fact, this result only shows that the non-linearity suppresses the large-amplitude pulse generation form the particular initial perturbation given by

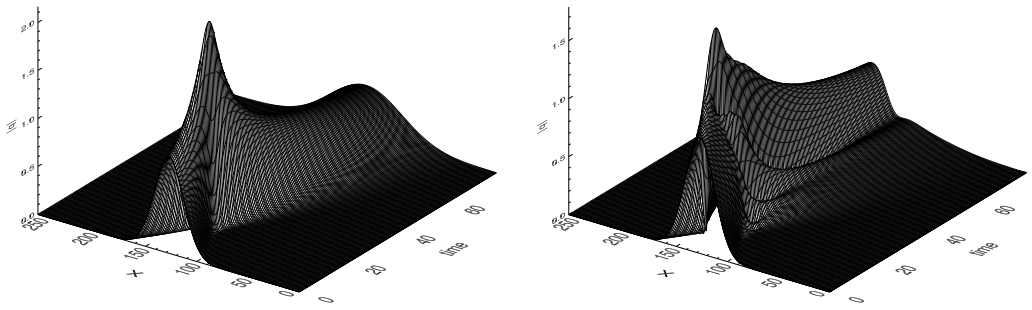

Fig. 4. The time evolution of the X-dependence of $|q|$ for $\sigma = 6$. The left panel corresponds to $N = 0$ (liner theory), and the right panel to $N = 0.45$. Figure taken from Ref. [43]

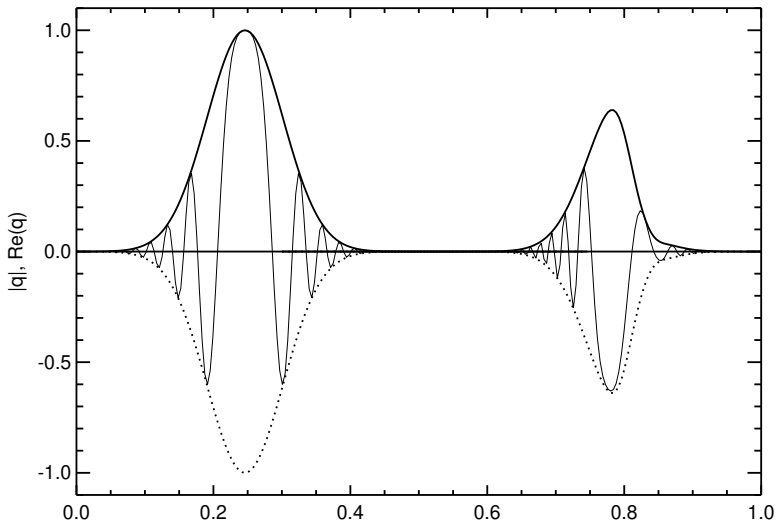

Fig. 5. The initial perturbations used in linear ($N = 0$) and nonlinear ($N = 0.45$) calculations. The thick and thin solid curves show $|q|$ and $\mathrm{Re}(q)$ respectively. The left curves correspond to (17) with $\sigma = 6$. Since equation (15) is invariant with respect to shift of x, the spatial positions of the initial perturbations are chosen arbitrarily. Figure taken from Ref. [43]

Eq. (17). It is quite possible that large-amplitude pulses can be generated from small-amplitude initial perturbations very efficiently even in the nonlinear regime if we change the initial condition. This conjecture was verified in the following way. Let $q_{\mathrm{lin}}(T, X)$ be the solution to Eq. (15) written in the dimensionless form with $N = 0$ and with the initial condition (17). It takes its maximum amplitude $(1 + \sigma^2)^{1/4}$ at $T = T_{\max} = \lambda t_{\max}/l^2$. Equation (15) was solved with $N = 0.45$ taking $q_{\mathrm{lin}}(T_{\max}, X)$ as the initial condition, and integrating it backward with respect to time. As a result, the solution $q_{\mathrm{nonl}}(T, X)$ was obtained for $T < T_{\max}$. Let $T = T_{\min} < T_{\max}$ be the moment of time when the amplitude of $q_{\mathrm{nonl}}(T, X)$ takes its minimum value. Then the solution to Eq. (15) with $N = 0.45$ and with the initial condition $q = q_0(X) \equiv q_{\mathrm{nonl}}(T_{\min}, X)$ at $T = 0$ is equal to $q_{\mathrm{lin}}(T_{\max}, X)$ at $T = T_{\max} - T_{\min}$. Fig. 5 displays $b_0(X)/a$ and $q_0(X)$ for $\sigma = 6$. We can see that $\max|q_0| < \max|b_0/a|$. Hence, the amplification rate obtained in the nonlinear regime with the initial perturbation q_0 is even larger than the amplification rate obtained in the linear regime with the initial perturbation (17). This example clearly shows that the dispersive focusing works both in nonlinear as well as in linear regime.

4 Summary and conclusions

In this paper we gave a brief review of the recent development in studying freak waves in plasmas. We started from considering the generation of ion-acoustic freak waves in plasmas with negative ions. When the concentration of negative ions is close to critical, the nonlinear ion-acoustic waves are described by the Gardner equation. The results of the numerical modelling of the time evolutions of modulationally unstable perturbations are discussed. These results clearly show that large-amplitude short-lived pulses are generated from the initial small-amplitude perturbation. These pulses have all typical properties of freak waves. The study of generation of freak ion-acoustic waves in plasmas with negative ions can be interesting for laboratory plasma experiments.

We then proceed to reviewing the study of generation of Alfvén freak waves in astrophysical plasmas. Nonlinear Alfvén waves propagating at small angles with respect to the background magnetic field are described by the DNLS equation. First we discussed the linear theory of the freak wave generation by the dispersive focusing. A simple solution of the linearized DNLS equation was presented. This solution shows that a wave group with the arbitrarily large ratio of amplitude to the amplitude of the initial perturbation can be obtained. Then we considered the freak wave generation in the nonlinear regime. The results of the numerical solution of the DNLS equation clearly show that the nonlinear dispersive focusing also results in the generation of large-amplitude short-lived Alfvénic pulses.

References

1. A.R. Osborne, M. Onorato and M. Serio, Phys. Lett. A **275**, (2000) 386-393
2. E. Pelinovsky, T. Talipova and C. Kharif, Physica D **147**, (2000) 83-94
3. A. Slunyaev, C. Kharif, E. Pelinovsky and T. Talipova, Physica D **173**, (2002) 77-96
4. C. Kharif and E. Pelinovsky, Eur. J. Mech. B Fluids **22**, (2003) 603-634
5. M. Hopkin, Nature **430**, (2004) 492-492
6. S. Perkin, Science News **170**, (2006) 328-329
7. C. Kharif, E.N. Pelinovsky and A. Slunyaev, *Rogue waves in the ocean*, Advances in Geophysical and Environmental Mechanics and Mathematics, Springer, (2009) 216 pp.
8. D.R. Solli, C. Ropers, P. Koonath and B. Jalali, Nature **450**, (2007) 1054-1058
9. D.-I. Yeom and B.J. Eggleton, Nature **450**, (2007) 953-954
10. L.F. Burlaga, N.F. Ness and M.H.Acuna, J. Geophys. Res. **112**, (2007) A07106
11. L.F. Burlaga and J.F. Lemaire, J. Geophys. Res. **83**, (1978) 5157-5160
12. B.T. Tsurutani, D. Southwood, E.J. Smith and A. Balogh, Geophys. Res. Lett. **19**, (1992) 1267-1270
13. D Winterhalter, M. Neugebauer, B.E. Goldstein, E.J. Smith, S. Bame and A. Balogh, J. Geophys. Res. **99**, (1994) 23371-23381
14. Y. Liu, J.D. Richadson, J.W. Beicher, J.C. Kasper and R.M. Skoug, J. Geophys. Res. **111**, (2006) A09108
15. K. Baumgärtel, J. Geophys. Res. **104**, (1999) 28295-28308
16. H. Washimi and T. Taniuti, Phys. Rev. Lett. **17**, (1966) 996-998
17. C.H. Su and C.S. Gardner, J. Math. Phys. **10**, (1969) 536-539
18. F. Tappert, Phys. Fluids **15**, (1972) 2446-2447
19. H. Ikezi, Phys. Fluids **16**, (1973) 1668-1675
20. S. Watanabe, J. Plasma Phys. **14**, (1975) 353-364
21. M.Q. Tran, Phys. Scripta **20**, (1979) 317-327
22. Y. Nakamura, IEEE Trans, Plasma Sci. **10**, (1982) 180-195
23. K.E. Lonngren, Plasma Phys. Control. Fusion **25**, (1983) 943-982
24. Y. Nakamura and I. Tsukabayashi, J. Plasma Phys. **34**, (1985) 401-415
25. S.G. Tagare, J. Plasma Phys. **36**, (1986) 301-312
26. F. Verheest, J. Plasma Phys. **39**, (1988) 71-79
27. B.C. Kalita and M.K. Kalita, Phys. Fluids B **2**, (1990) 674-676
28. B.C. Kalita and G.C. Das, J. Phys. Soc. Japan **71**, (2002) 2918-2024
29. Y. Nakamura J.L. Ferreira and G.O. Ludwig, J. Plasma Phys. **33**, (1985) 237-248

30. S. Watanabe, J. Phys. Soc. Japan **53**, (1984) 950-956
31. M.S. Ruderman, T. Talipova and E. Pelinovsky, J. Plasma Phys. **74**, (2008) 639-656
32. R. Grimshaw, E. Pelinovsky, T. Talipova, M.S. Ruderman and R. Erdélyi, Studies Appl. Math. **114**, (2005) 189-210
33. E.J. Parkes, J. Phys. A **20**, (1987) 2025-2036
34. R. Grimshaw, D. Pelinovsky, E. Pelinovsky and T. Talipova, Physica D **159**, (2001) 35-57
35. T.R. Benjamin and I.F. Feir, J. Fluid Mech. **27**, (1967) 417-430
36. A.C.Newell, *Solutons in Mathematics and Physics* (Philadelphia, PA: SIAM, 1985)
37. Y.A. Berezin, *Modelling Nonlinear Wave Processes* (Utrecht: VNU Science Press, 1987)
38. A. Rogister, Phys. Fluids **14**, (1971) 2733-2743
39. E. Mjølhus, J. Plasma Phys. **16**, (1976) 321-334
40. K. Mio, T. Ogino, K. Minami, S. Takeda, J. Phys. Soc. Jpn. **41**, (1976) 265-271
41. E. Mjølhus, T. Hada, in: *Nonlinear Waves and Chaos in Space Plasmas*, edited by T. Hada, H. Matsumoto, Terrapub, Tokio (1997) 121-169
42. S.P. Spangler, in: *Nonlinear Waves and Chaos in Space Plasmas*, edited by T. Hada, H. Matsumoto, Terrapub, Tokio (1997) 171-223
43. V. Fedun, M.S. Ruderman and R. Erdélyi, Phys. Lett. A **372**, (2008) 6107-6110
44. D.J. Kaup and A.C. Newell, J. Math. Phys. **19**, (1978) 798-801
45. T. Kawata and H. Inoue, J. Phys. Soc. Jpn. **44**, (1978) 1968-1976
46. M. Wadati, K. Konno and Y.H. Ichikawa, J. Phys. Soc. Jpn. **46**, (1979) 1965-1966
47. T. Kawata, J. Sakai and N. Kobayashi, J. Phys. Soc. Jpn. **48**, (1980) 1371-1379
48. X.J. Chen, H.L. Wangand W.K. Lam, Phys. Let. A **353**, (2006) 185-189
49. X.J. Chen, J. Yang and W.K. Lam, J. Phys. A **39**, (2006) 3263-3274
50. V.M. Lashkin, J. Phys. A **40**, (2007) 6119-6132
51. G.Q. Zhou and N.N. Huang, J. Phys. A **40**, (2007) 13607-13623